BIOCHEMISTRY
including biophysical chemistry & molecular biology

Article

pubs.acs.org/biochemistry

A Red/Green Cyanobacteriochrome Sustains Its Color Despite a Change in the Bilin Chromophore's Protonation State

Chen Song,[†,‡] Francisco Velazquez Escobar,[§] Xiu-Ling Xu,[∥] Rei Narikawa,[⊥,#,@] Masahiko Ikeuchi,[⊥,▽] Friedrich Siebert,[§] Wolfgang Gärtner,[∥] Jörg Matysik,*[,‡] and Peter Hildebrandt*[,§]

[†]Leids Instituut voor Chemisch Onderzoek, Universiteit Leiden, 2300 RA Leiden, The Netherlands

[‡]Institut für Analytische Chemie, Universität Leipzig, Linnéstraße 3, D-04103 Leipzig, Germany

[§]Technische Universität Berlin, Institut für Chemie, Sekr. PC14, Straße des 17. Juni 135, D-10623 Berlin, Germany

[∥]Max-Planck-Institut für Chemische Energiekonversion, Stiftstraße 34−36, D-45470 Mülheim an der Ruhr, Germany

[⊥]Department of Life Sciences (Biology), Graduate School of Art and Sciences, University of Tokyo, Komaba 3-8-1, Meguro, Tokyo 153-8902, Japan

[#]Department of Biological Science, Faculty of Science, Shizuoka University, Shizuoka 422-8529, Japan

[@]Precursory Research for Embryonic Science and Technology (PRESTO), Meguro, Tokyo 153-8902, Japan

[▽]Japan Science and Technology Agency (JST), Core Research for Evolutionary Science and Technology (CREST), Meguro, Tokyo 153-8902, Japan

Supporting Information

ABSTRACT: The second GAF domain of AnPixJ, AnPixJg2, a bilin-binding protein from the cyanobacterium *Anabaena* PCC 7120, undergoes a photoinduced interconversion between a red-absorbing state, Pr, and a green-absorbing state, Pg. Combining ultraviolet−vis (UV−vis), infrared, resonance Raman (RR), and magic-angle spinning (MAS) nuclear magnetic resonance (NMR) spectroscopy, we have studied this cyanobacteriochrome (CBCR) assembled with phycocyanobilin (PCB) either *in vivo* or *in vitro*. In both assembly routes, the spectroscopic data of the Pr state reveal nearly identical chromophore structures with a protonated (cationic) bilin. However, unlike the native (*in vivo* assembly) Pg photoproduct, in which the bilin retains protonation, the Pg generated from the *in vitro*-assembled AnPixJg2 harbors a deprotonated (neutral) bilin chromophore at pH 7.8. IR difference spectroscopy further reveals the transfer of a proton from the bilin to a side-chain carboxylate on an amino acid, probably Asp291. Besides the change in protonation state, the bilin structure is very similar in the *in vitro*- and *in vivo*-assembled Pg photoproducts. The chromophore of the *in vitro* Pg becomes protonated when the pH is increased to 10, presumably because of a partial reversal of protein misfolding. Most remarkably, the electronic transitions remain unchanged and are very similar to those of the native Pg. Thus, bilin protonation is not a key parameter for controlling the energies of the electronic transitions in AnPixJg2. Possible alternative molecular mechanisms for color tuning are discussed.

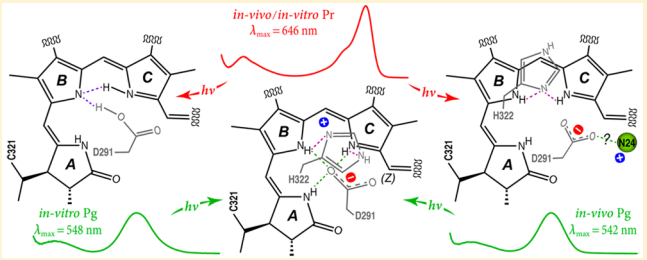

Biological photoreceptors are outstandingly optimized for their functions by a precise interaction between the protein moiety and the embedded chromophore. In particular, tuning of spectral sensitivity demonstrates the essential role of the protein environment for the chromophore properties, as has been exemplified in great detail for two classes of photoreceptors, the mammalian and microbial retinal-binding receptors[1] as well as the bilin-binding receptors such as phytochromes and the more recently identified functionally related cyanobacteriochromes (CBCRs).[2,3]

CBCRs display a remarkable spectral variability. Many of these proteins are generated as a red-absorbing dark state, Pr, spectrally very similar to that of canonical (cyanobacterial) phytochromes, whereas their photoproducts cover a wide spectral range from 750 to 400 nm.[4−8] Such a broad spectral variety is also found for the retinal Schiff base in vertebrate rhodopsins where the absorption properties are known to be mainly controlled via the variations of the electrostatics in the bilin-binding pocket.[1] For color tuning in CBCRs, however, various effects are under discussion. The bilin can be reversibly converted from PCB into phycoviolobilin (PVB) via a cysteine-mediated reaction, resulting in a reduced length of the bilin conjugated π-electron system, and even rubinoid chromophores can be formed via the formation of a transient bond between a

Received: January 19, 2015
Revised: August 20, 2015
Published: September 3, 2015

DOI: 10.1021/acs.biochem.5b00735
Biochemistry 2015, 54, 5839−5848

second cysteine and the bilin C10 atom.[9−11] A reduction of the conjugation length is also possible via geometric distortion of the tetrapyrrole, following the photoisomerization at the **C−D** methine bridge. This has been shown for the green-absorbing photoproduct of the red/green CBCR from *Nostoc punctiforme* where Phe residues stabilize a nearly perpendicular orientation of ring **D** with respect to the rest of the chromophore.[12,13] This concept implies that, in the Pr state, the **D** ring participates in the conjugation, whereas for its photoproduct, rotation around the 14,15-single bond, stabilized by the protein matrix (most likely the aromatic residues in close contact with the **D** ring[14]), disconnects this ring from the π-electron system. Another recent NMR spectroscopic study of the red/green CBCR NpR6012g4 from *N. punctiforme* points to additional structural changes at the **C−D** and **B−C** methine bridges concomitant to the formation of the green-absorbing state.[15] For the native AnPixJg2, some of us have suggested that the substantial blue shift of the absorption maximum upon formation of the Pg state is due to the influx of water molecules into the chromophore pocket, brought about by the *Z*-to-*E* isomerization of the **C−D** methine bridge.[16]

CBCRs often are composed of arrays of several GAF (c**G**MP phosphodiesterase/**a**denylyl cyclase/**F**hlA) domains.[2] It has, however, been demonstrated that already autonomously expressed GAF domains from CBCRs fold in a functional manner. They are able to bind PCB as the chromophore and to show remarkable photochromic absorbance shifts following photochemical processes similar to those in canonical phytochromes.[12] Among the best-studied CBCR GAF domains is the second GAF domain of red/green-type CBCR AnPixJ (AnPixJg2) from the cyanobacterium *Anabaena* (*Nostoc*) sp. PCC 7120, for which the three-dimensional structure of its red-absorbing parental state (Pr) is available.[10] Moreover, the photocycle has been studied by optical and vibrational spectroscopies.[16,17] This GAF domain undergoes photochromicity between Pr (648 nm) and a light-induced green-absorbing state, here in brief denoted as the photoproduct (Pg, 542 nm). The Pg photoproduct shows moderate thermal stability and can fully revert into the parental state by irradiation with light of the appropriate wavelength. Both photoinduced routes involve double-bond isomerization around the **C−D** methine bridge and a transient deprotonation of the chromophore during photoconversion;[16,17] the final product of the photochemical process leads to protonated chromophore with a *ZZZssa* and *ZZEssa* geometry as Pr and Pg, respectively.[15,16]

In this work, we have revisited the photochemical process of AnPixJg2 by extending the studies to the *in vitro*-assembled holoprotein variant using infrared (IR), RR, and MAS NMR spectroscopy. This reinvestigation was prompted by initially contradictory results obtained from MAS NMR and vibrational spectroscopy. In contrast to the *in vivo*-assembled (native) holoprotein used in previous IR and RR studies,[16,17] *in vitro* assembly (required for selective isotope labeling of the bilin for NMR measurements) afforded a modified ground-state structure of the bilin-binding pocket as reflected by a deprotonated (neutral) tetrapyrrole in the Pg state. Whereas this structural perturbation is already surprising, it is even more puzzling that the electronic absorption band is hardly altered by the change in bilin protonation.

MATERIALS AND METHODS

***In Vitro* Reconstitution.** Expression and purification of AnPixJg2 apo- and holoprotein as well as *in vivo* ^{15}N labeling of the PCB chromophore are described in the text of the Supporting Information. For *in vitro* reconstitution, PCB was isolated from *Spirulina platensis* as described previously.[18] [$^{15}N_4$]PCB was kindly provided by J. Hughes (Gießen). Stock solutions of PCB(s) were prepared in dimethyl sulfoxide, and aliquots of the stock solution were added to the AnPixJg2 apoprotein to give final concentrations of ∼20 μM PCB and 10 μM apoprotein in buffer B. The mixture was incubated in the dark at 4 °C overnight. The reconstituted proteins were purified by a second Ni affinity chromatography. For pH-dependent measurements, both *in vivo*- and *in vitro*-reconstituted proteins were prepared at pH 6.0 (100 mM Mes·NaOH), pH 7.8 (50 mM Tris, 300 mM NaCl, and 5 mM EDTA), and pH 10.0 (100 mM glycine·NaOH).[19]

MAS NMR Data Collection. Prior to the NMR measurement in the Pr state, the protein was loaded into a 1 mm bore glass capillary syringe at 20 °C and illuminated with 525 nm light for 2 min from an array of appropriate LEDs to ensure full photoconversion.[5] We note that the remaining fraction of green-absorbing photoproduct was negligible for the NMR measurements. A similar strategy for converting the sample from Pr to Pg form was used under illumination of red light at 650 nm.

All ^{15}N CP (cross-polarization)-MAS experiments were performed on a Bruker AV-750 WB spectrometer equipped with a 4 mm triple-resonance MAS probe. Approximately 1.8 mg of *in vitro*-assembled and 1.6 mg of *in vivo*-assembled holoproteins of AnPixJg2 were used in this study. Each sample was loaded into a 4 mm zirconia MAS rotor and cooled to −40 °C in the magnet. The MAS spectra of the *in vivo*-assembled sample were acquired at a MAS rate of 13 kHz, and the *in vitro*-assembled sample was measured successively at 13, 6.5, and 5.5 kHz. Typical ^{1}H $\pi/2$ and ^{15}N π pulses were 3.2 and 8.5 μs, respectively. ^{15}N transverse magnetization created by the ramped CP was transformed from ^{1}H with an optimal contact time of 4.096 ms for the *in vivo*-assembled sample, and three CP contact times of 1.024, 4.096, and 8.192 ms were used for *in vitro*-assembled sample. The optimal contact time was found to be 4.096 or 8.192 ms for the *in vitro* sample in its Pr or Pg photoproduct state, respectively. For ^{1}H decoupling, a two-pulse phase modulation scheme with a pulse duration of 5.5−7 μs and a ^{1}H radiofrequency field strength of 80 kHz was employed. All spectra were recorded with 90k scans with a recycle delay of 1.5 s unless otherwise stated. A Lorentzian apodization function with a line broadening factor of 75 Hz was applied to data processing. Data were preprocessed with Topspin 3.1 (Bruker BioSpin, Rheinstetten, Germany). All 13 kHz AnPixJg2 spectra were subsequently fitted to the Voigt line shape for peak areas (Figure S1 of the Supporting Information), and the Pg spectra of the *in vitro*-assembled AnPixJg2 obtained at 6.5 and 5.5 kHz were transferred to program *dmfit*[20] for determination of the chemical shift anisotropy (CSA) tensors (Figure S2 of the Supporting Information).

Vibrational Spectroscopy. Details of the RR experiments were described previously.[16] In addition to measurements under standard RR cryogenic conditions (−140 °C) and for direct comparison with NMR results, RR measurements of both states of the *in vitro*-assembled sample were also conducted at −40 °C.

DOI: 10.1021/acs.biochem.5b00735
Biochemistry 2015, 54, 5839−5848

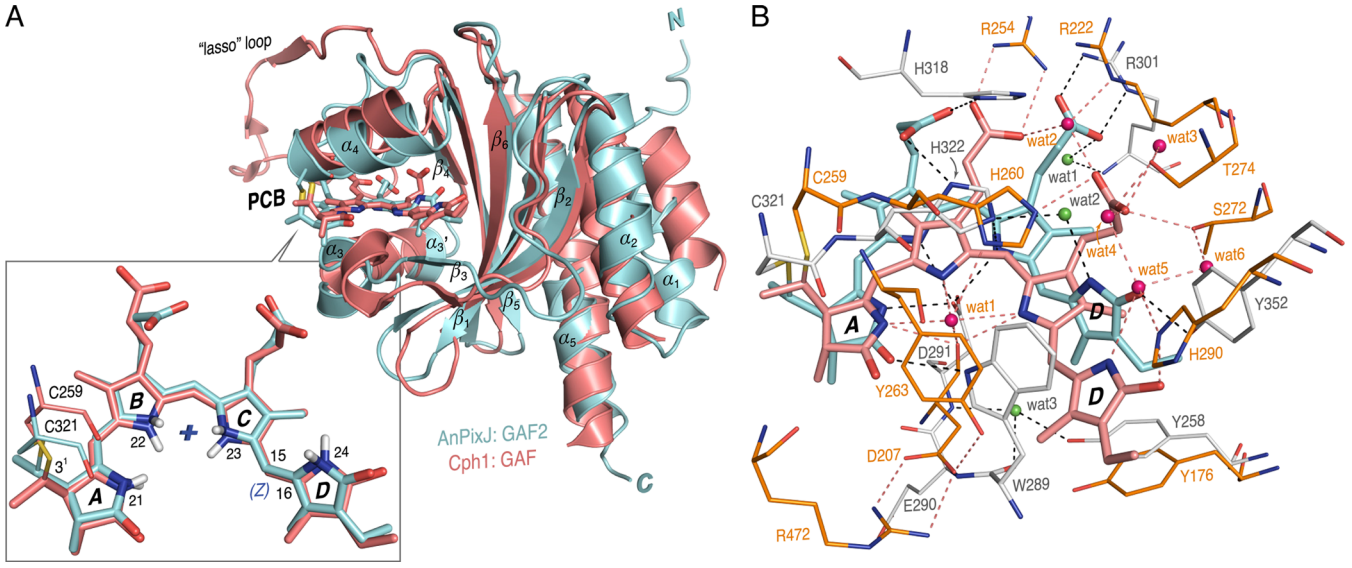

Figure 1. Structural comparison of the GAF domain from AnPixJ and Cph1 in the red-absorbing Pr state. (A) Superposition of AnPixJg2 3W2Z (cyan) and Cph1 2VEA (brown) structures. The central α-helices and β-sheet are labeled according to AnPixJg2 convention. The respective PCB chromophores are shown as sticks using the same color coding as for the ribbon diagrams. Superimposed bilins are enlarged and displayed as the inset, in which both adopt the 15*Za* geometry covalently ligated to the S^{γ} atom of a Cys (C321 and C259 in AnPixJg2 and Cph1, respectively) via its ethylidene group of ring **A** ($C3^{1}$). Four pyrrole rings **A**–**D** and their nitrogens are labeled for reference. (B) Structural views of the PCB-binding pocket in AnPixJg2 (PCB, cyan, and amino acids, gray) and in Cph1 (PCB, brown, and amino acids, orange). Interactions between the bilin and nearby amino acids are indicated by dashed lines (black and orange for AnPixJg2 and Cph1, respectively). Water molecules in the tetrapyrrole cavities of AnPixJg2 and Cph1 are marked as green and pink spheres, respectively.

IR measurements were performed in an IFS-28 spectrometer (Bruker Optics) equipped with an MCT detector and a home-built cryostat. The sample solution was concentrated under a moderate N_2 gas flow on a CaF_2 window with a 2 μm deepening. The concentration of the protein microfilm was around 0.5−1 mM. Subsequently, the sample was covered with a plain CaF_2 window. To avoid dehydration during the measurement, the sample sandwich was sealed with silicone grease. IR measurements were performed at room temperature. As in the RR measurements, photoconversion between the two photostates was achieved by irradiation by either red (670 nm) or green (530 nm) light from an array of LEDs. Further experimental details are given elsewhere.[16]

RESULTS

MAS NMR Spectroscopy of AnPixJg2 in the Pr State. The crystal structure of AnPixJg2 in its Pr state [Protein Data Bank (PDB) entry 3W2Z][10] revealed an overall structural similarity to that of the GAF domains in canonical phytochromes, e.g., Cph1 (PDB entry 2VEA for its complete sensory module, Cph1Δ2)[21] (Figure 1). This is particularly true for the tetrapyrrole geometry as demonstrated by the good agreement of the RR spectra.[16] Also, the MAS NMR Pr spectra of the ^{15}N-labeled PCB for both preparations of AnPixJg2, i.e., *in vitro* and *in vivo* PCB assembly (Figure 2C,E), display far-reaching similarities with Cph1Δ2 (Figure 2A). The complete assignment of the ^{15}N signals of the PCB chromophore in Cph1Δ2 (for a review, see ref 22) thus forms the basis for assignment of the corresponding Pr spectra of AnPixJg2 (Table S1 and Text of the Supporting Information). Spectral fitting analysis of two AnPixJg2 Pr spectra is shown in Figure S1A,C of the Supporting Information. If the spectrum obtained from the *in vitro*-assembled sample is taken as an example (Figure S1A of the Supporting Information), peaks can directly be quantified by a Voigt line-shape spectral model function, yielding a ratio of 1.9:1.0:1.0 for three maxima at 155.8, 144.9, and 133.7 ppm. Such a narrow dispersion of ^{15}N shifts, as also seen in both photostates of Cph1Δ2 (Figure 2A,B), provides conclusive evidence that all four bilin nitrogens of AnPixJg2 in the Pr state are protonated and thus the chromophore carries a positive charge (not considering both dissociated propionates of rings **B** and **C**).[23,24] The same conclusion holds for the *in vivo*-assembled Pr state AnPixJg2 (Figure 2E as well as Figure S1C and Table S1 of the Supporting Information). Additionally, all ^{15}N Pr signals of AnPixJg2 occur at δ^{N} positions close to those observed for Cph1Δ2 [$|\Delta\delta^{N}| \leq 4.9$ ppm (Table S1 of the Supporting Information)], indicating that the positive charge held by the tetrapyrrole system is similarly distributed in both photosensors in their parental states. For the Pr state, assignments of the ^{15}N chemical shifts agree also with those recently reported for the Pr state of the related CBCR NpR6012g4 using solution NMR spectroscopy[15] (for comparison, see Table S1 of the Supporting Information).

RR Spectroscopy of AnPixJg2 in the Pr State. Also, the RR spectra of the Pr state are nearly identical for the *in vivo* and *in vitro* AnPixJg2 preparations (Figure 3B as well as Figures S3A and S6A,B of the Supporting Information). The only detectable differences in the spectrum of *in vitro* Pr refer to slight frequency upshifts of the weak bands at 1247, 1277, and 1290 cm^{-1} (Figure S3A of the Supporting Information). Even though the assignment of these bands is not entirely clear, these spectral changes likely reflect only subtle conformational differences of the bilins in both preparations. In both cases, the vibrational band pattern is characteristic of a *ZZZssa* bilin geometry,[16] in line with the crystallographic data.[10] Moreover, the bilin ring system is cationic with all four pyrrole nitrogens fully protonated as specifically indicated by the N−H in-plane bending mode (N−H i.p.) of ring **B** and **C** pyrrole nitrogens at 1580 cm^{-1}. Upon H/D exchange, this band undergoes a downshift to ~1070 cm^{-1}, consistent with an essentially pure

DOI: 10.1021/acs.biochem.5b00735
Biochemistry 2015, 54, 5839−5848

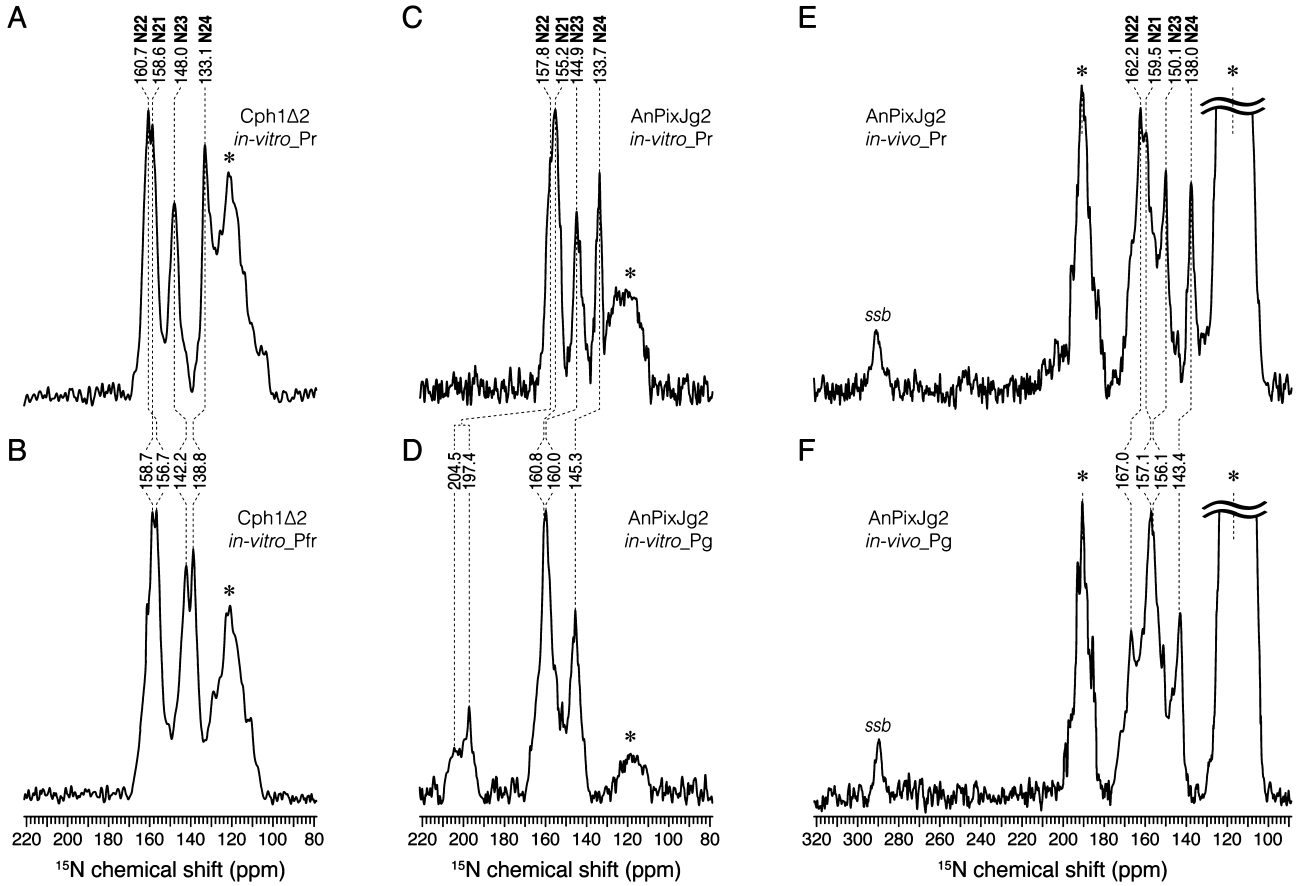

Figure 2. ^{15}N CP-MAS NMR spectra of Cph1Δ2 and AnPixJg2 containing isotopically labeled PCB. For ^{15}N spectra of Cph1Δ2 in its red-absorbing dark state (Pr, A) and the far-red-absorbing photoproduct (Pfr, B), ∼10 mg holoproteins generated by *in vitro* assembled with [U-^{13}C,^{15}N]PCB were used.[44] Data acquisition parameters were the same as for the AnPixJg2 spectra shown in panels C−F except for a CP contact time of 2.048 ms and 20K scans (for details on AnPixJg2 data collection, see Materials and Methods). (C−F) Spectra of the AnPixJg2 holoproteins after *in vitro* (C and D) or *in vivo* (E and F) assembly with [^{15}N$_4$]PCB in the Pr state (C, *in vitro*, and E, *in vivo*) and in the Pg state (D, *in vitro*, and F, *in vivo*). ^{15}N chemical shifts (δ^N) are indicated by the vertical lines. Peak assignment for Cph1Δ2 in both photostates is based on ref 22, and for the two AnPixJg2 samples, see the main text. Signals marked with an asterisk originate from the amide nitrogens of the protein backbone in natural abundance (A−D); for the *in vivo* spectra (E and F), the protein signals arising from backbone amide (centered at ∼120 ppm, chopped off at the same fixed height) and His imidazoles (∼188 ppm) due to ^{15}N incorporation are denoted by asterisks. ^{15}N chemical shifts were externally referenced to the N$^{\alpha}$ signal of histidine·HCl at 49.04 ppm on the liquid NH$_3$ scale.

N−H i.p. mode.[16] In both the *in vivo* and *in vitro* preparations, the Pr chromophore remains protonated in the pH range from 6.0 to 10.0, although the variation of the N−H i.p. frequency is slightly different for both samples. In view of the sensitivity of this mode with respect to hydrogen bond interactions,[25] these findings reflect only slight differences in the hydrogen bond network of the *in vivo* and *in vitro* Pr states. Except for the N−H i.p. mode, the RR spectra of the *in vivo* and *in vitro* Pr states are very similar in this pH range. However, compared to the *in vivo* Pr form, the *in vitro* Pr counterpart seemed to be less stable in acidic medium, as indicated by changes in the absorption spectrum (Figure 3A).

MAS NMR Spectroscopy of AnPixJg2 in the Pg State. Investigation of the AnPixJg2 Pg photoproducts obtained from both preparation protocols yielded a more complex picture. Inspection of the pyrrole nitrogen signals for the photoproduct of the *in vivo* PCB-loaded sample indicates that the bilin remains fully protonated as in its Pr state, evidenced by all four pyrrole signals resonating below 167.0 ppm with a narrow δ^N dispersion of ∼23 ppm (Figure 2F and Figure S4 of the Supporting Information for the full spectrum). This demonstrates that the native species carries a protonated bilin in both photostates. In this respect, the results are similar to those reported for the Pg state of the related red/green CBCR NpR6012g4,[15] although in the latter the peak of the **D**-ring nitrogen was observed at a distinctly lower field (Table S1 of the Supporting Information).

In contrast, the spectrum of the *in vitro*-generated Pg state (Figure 2D) exhibits distinct spectral features, referring to the appearance of broad and low-intensity signals at 197.4 ppm with a downfield shoulder at 204.5 ppm that can reasonably be attributed to a deprotonated bilin, supported by the following arguments. (i) A marked downfield shift with respect to all δ^N is observed for a protonated bilin in both photostates of Cph1Δ2 and native AnPixJg2 (see below and Table S1 of the Supporting Information). Deprotonated nitrogens in porphyrins,[26] verdinoid bile pigments,[27] and pheophytins[28] show signals in the low-field region above 220 ppm. Also, the signal for the unprotonated **B**-ring nitrogen of free PCB is found at 260.8 ppm in the crystalline state and 245.5 ppm in solution.[29] (ii) Voigt deconvolution of the spectrum measured with a CP contact time of 8.192 ms reveals an imbalanced intensity ratio of 0.7:1.7:1.0 for the three maxima at around 197.4, 160.2, and 145.3 ppm (Figure S1B of the Supporting Information). The

DOI: 10.1021/acs.biochem.5b00735
Biochemistry 2015, 54, 5839−5848

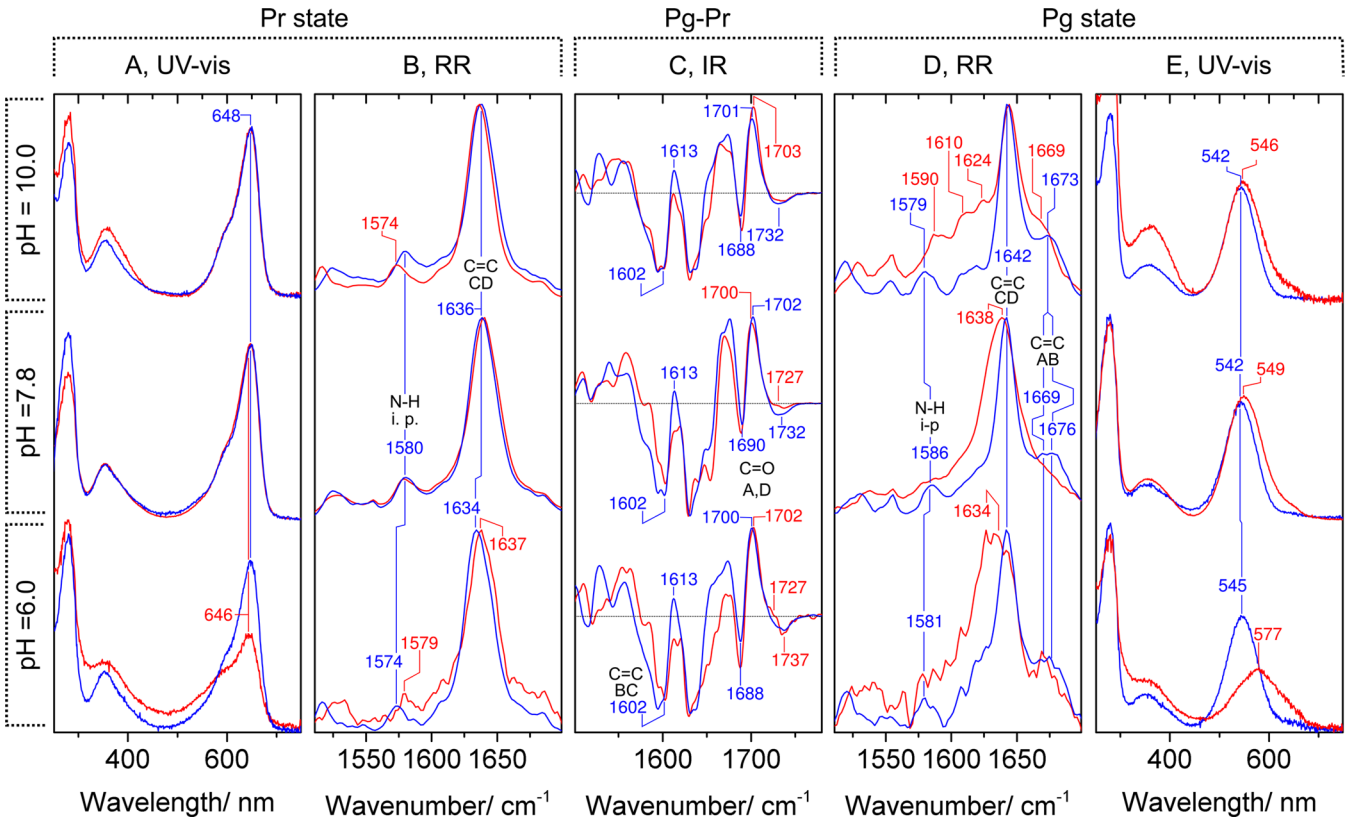

Figure 3. UV−vis absorption, RR, and IR spectra of AnPixJg2 assembled *in vivo* (blue) and *in vitro* (red), measured at different pH values: (A) UV−vis absorption spectra of the Pr state, (B) RR spectra of the Pr state, (C) Pg-minus-Pr IR difference spectra, (D) RR spectra of the Pg state, and (E) UV−vis absorption spectra of the Pg state.

observed loss of peak intensities is most likely due to the slow CP normally seen in proton-poor regions.[30] (iii) The low-field signals are notably reduced at the shorter contact times of 1.024 and 4.096 ms instead of 8.192 ms (Figure S5B of the Supporting Information), while the signals below 160.8 ppm exhibit similar intensities at 1.024 and 8.192 ms but increase slightly at 4.096 ms (Figure S5B of the Supporting Information), characteristic of protonated pyrrole nitrogens as in the Pr state (Figure S5A of the Supporting Information). This implies that the low-field signals, presumably originating from an unprotonated bilin nitrogen, have a distinct $^{1}H \rightarrow {}^{15}N$ CP kinetics with the directly protonated nitrogens, possibly due to weaker N···H interactions.[31] (iv) At least two sets of spinning sidebands spaced at 5.5 or 6.5 kHz are observed for the low-field signals (Figure S2 of the Supporting Information), while for the protonated nitrogen sites below 160.8 ppm, sidebands are not clearly visible at the MAS rate of 5.5 kHz (Figure S2A of the Supporting Information) and are absent at 6.5 kHz (Figure S2B of the Supporting Information); this leads to a much larger span of ^{15}N CSA tensors ($\Omega_{cs} > 210$ ppm) and a reduced asymmetry parameter ($\eta_{cs} < 0.3$) for the low-field signals (Figure S2 of the Supporting Information, inset). These anisotropy values agree with those reported for unprotonated imidazole nitrogens, carrying a free lone pair, as in BChl *a*/His complexes,[30] histidine-containing peptides,[32] and histidine itself as studied in great detail on various tautomeric and protonation states.[29] Hence, there is unquestionable MAS NMR evidence of a deprotonated bilin in its Pg state of the *in vitro*-prepared sample.

The three other ^{15}N signals are downfield-shifted by at least 5.6 ppm (Table S1 of the Supporting Information), indicating that the loss of positive charge upon deprotonation affects the entire bilin. Two ^{15}N signals are less affected and are thus assigned to the terminal positions of N21 and N24. Following Occam's razor, these terminal nitrogens shift to 160.8 or 160.0 ppm (N21, from 155.2 ppm as Pr) and to 145.3 ppm (N24, from 133.7 ppm as Pr). Following the same argument, N23 would shift to 160.0 or 160.8 ppm (from 144.9 ppm as Pr), and the deprotonated signal would originate from N22, corresponding to a downshift of ∼45 ppm. Moreover, according to MAS data for the protonation shift of PCB upon its assembly into apo-Cph1Δ2,[33] N22 of pyrrole ring **B** appears to be a more plausible candidate than N23 for the low-field deprotonated signals. Hence, we tentatively assign the downfield signals of the deprotonated nitrogen to N22 of ring **B**. The downfield shift of the N22 signal can be understood in terms of its deprotonation, and the origin of its split and slight broadening (Figure S1B and Table S1 of the Supporting Information) may reflect two discrete substates in which the **B**-ring nitrogen is involved in different hydrogen bonding interactions with the binding pocket. These interactions might involve not only Asp291 (AnPixJ numbering of residues is used throughout the article) but also His322 in close contacts with bilin rings **A**−**C** (Figure 1B) and the large number of water molecules that have entered the pocket in the Pg state, as implied by the previous RR study.[16]

RR Spectroscopy of AnPixJg2 in the Pg State. For *in vivo*-assembled holo-AnPixJg2 at pH 7.8, the RR spectrum for the Pg photoproduct displays a band pattern similar to that of Pfr states of canonical phytochromes, except for a systematic frequency upshift of all bands above 1550 cm^{-1}. As discussed in detail previously, we thus assigned the bilin structure to a

DOI: 10.1021/acs.biochem.5b00735
Biochemistry 2015, 54, 5839−5848

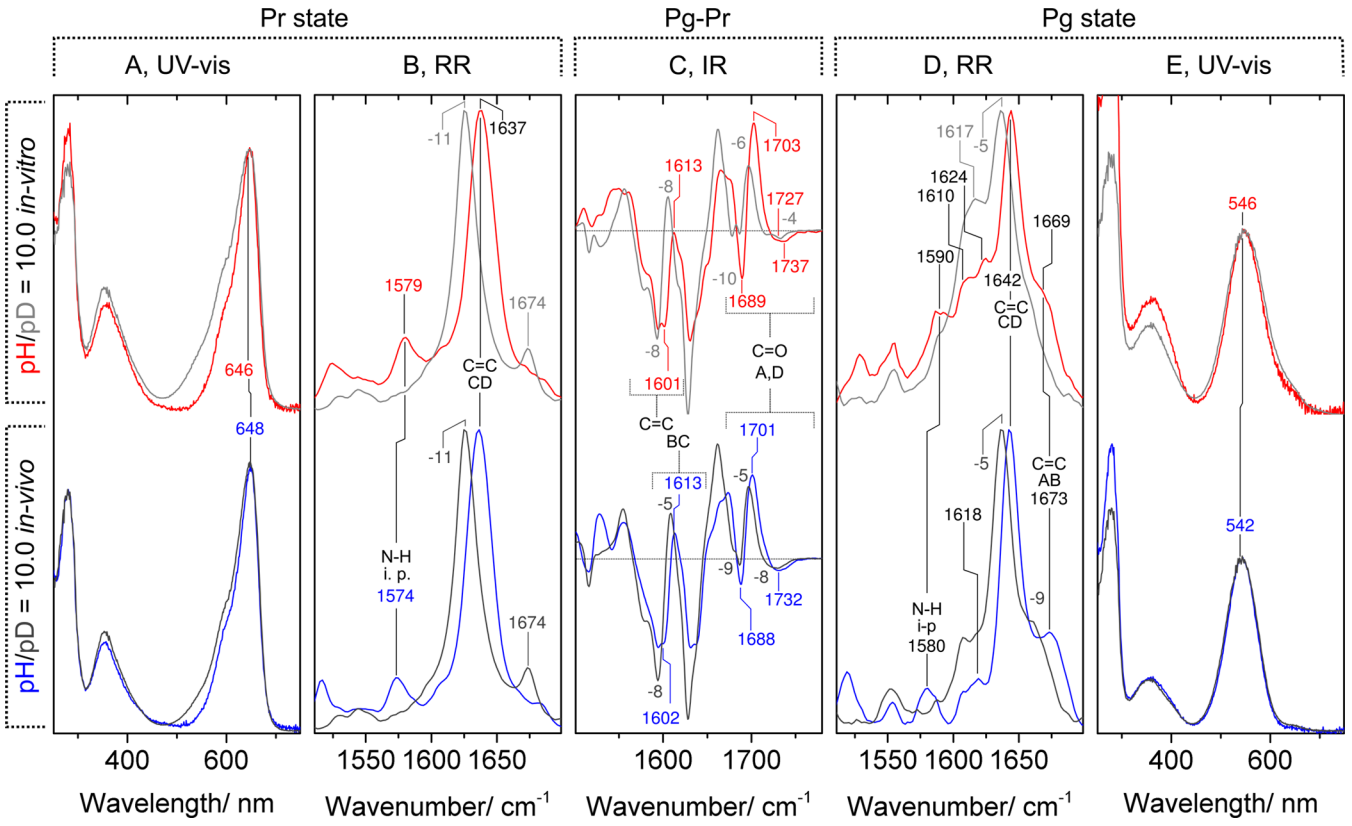

Figure 4. UV−vis absorption, RR, and IR spectra of AnPixJg2 assembled *in vivo* (blue) and *in vitro* (red), measured at pH 10.0 and pD 10.0: (A) UV−vis absorption spectra of the Pr state, (B) RR spectra of the Pr state, (C) Pg-minus-Pr IR difference spectra, (D) RR spectra of the Pg state, and (E) UV−vis absorption spectra of the Pg state. Gray traces refer to the spectra measured in D_2O.

protonated (cationic) tetrapyrrole in the *ZZE* configuration.[16] The unique marker band for the protonated form, the N−H i.p. of the **B**- and **C**-pyrrole nitrogens, is observed at 1586 cm^{-1}.[16] This mode is preserved albeit at slightly different positions between pH 6.0 and 10.0 (Figure 3D), reflecting changes in the hydrogen bond network similar to the Pr state (Figure 3B). Most importantly, this band is absent in the corresponding Pg spectrum of the *in vitro*-assembled sample at pH 7.8, and in acidic solutions down to pH 6.0, the chromophore remains deprotonated (Figure 3D and Figure S6C,D of the Supporting Information). Concomitantly, the strongest band, originating from the C═C mode of the **C−D** methine bridge, is downshifted to 1638 cm^{-1} and considerably broadened, which may reflect the conformational heterogeneity as also revealed by MAS NMR. Moreover, the high-frequency bands at 1669 and 1676 cm^{-1}, observed for the *in vivo* Pg (Figure 3D), have lost intensity and may just contribute to the high-frequency wing of the broad and asymmetric 1638 cm^{-1} envelope in the *in vitro* Pg spectrum. The resultant poorly structured band pattern in the region between 1550 and 1680 cm^{-1} is consistent with those of unprotonated tetrapyrroles because of the overlapping contributions of the tautomeric **B**- and **C**-deprotonated species. The deprotonation of either ring **B** or ring **C** and the concomitant structural changes of the bilin are also reflected in the other regions of the spectrum (Figure S3C,D of the Supporting Information). Note that the same results were obtained from AnPixJg2 assembled with the ^{15}N-labeled PCB chromophore and upon measuring the spectra at −40 °C, corresponding to the sample and conditions of the NMR measurements (Figure S6 of the Supporting Information).

Most surprisingly, however, the Pg state of the *in vitro* preparation shows a different picture in an alkaline solution. Here, the RR spectrum shows a set of well-resolved bands, including a sharp peak at 1642 cm^{-1}, which is at the same position as the *C−D* stretching mode of the Pg state of the *in vivo* preparation (Figure 3D). Moreover, also the N−H i.p. bending at 1580 cm^{-1} (Pg, *in vivo*) seems to have a counterpart in the spectrum of the *in vitro* Pg, albeit at an upshifted position at 1590 cm^{-1}. This is in fact confirmed by the disappearance of this band in D_2O (pD 10.0). Also, the *C−D* stretching mode reveals the same isotopic effect as observed for *in vivo* Pg [−5 cm^{-1} (Figure 4)]. Despite these similarities, the RR spectrum of *in vitro* Pg displays additional and weakly H/D-sensitive bands that are not present in the RR spectrum of the *in vivo* Pg (Figure 3D and Figure S4). We thus conclude that at pH 10.0 the *in vitro* Pg exists in a mixture of a protonated and deprotonated chromophore. However, the protonated chromophore does not possess the same structure as its *in vivo* counterpart. Among other indications, we specifically note the distinctly higher N−H i.p. bending frequency (1590 cm^{-1} vs 1580 cm^{-1}) that reflects much weaker hydrogen bond interactions.[25]

IR Difference Spectroscopy. The Pg-minus-Pr difference spectra of the *in vivo*- and *in vitro*-assembled samples (Figure 3C and Figure S3C of the Supporting Information) lack distinct amide I difference signals, thereby ruling out major secondary structural changes in both preparations as observed in canonical phytochromes.[19] The small differences in the amide I (1620−1680 cm^{-1}) and amide II (1530−1570 cm^{-1}) regions, however, demonstrate the minor changes in the overall protein structure between the *in vivo* and *in vitro* preparations. The IR data

DOI: 10.1021/acs.biochem.5b00735
Biochemistry 2015, 54, 5839−5848

further allow the exploration of the C=O stretching modes of the PCB chromophore. In the *in vivo* preparation, a strong difference signal (Pg, positive; Pr, negative) is observed at 1702/1690 cm^{-1} that can be assigned to the **D**-ring carbonyl.[34,35] This band pair is only slightly affected (±2 cm^{-1}) upon variation of the pH. For the corresponding C=O stretching of ring **A**, only the Pr mode can readily be identified as the negative band at 1732 cm^{-1}, whereas its counterpart in Pg is presumably obscured by the high-frequency wing of the 1702 cm^{-1} band. Here, the *in vitro* sample displays a different picture because the negative 1732 cm^{-1} band seems to be superimposed by a positive band at nearly the same position (~1727 cm^{-1}). This new positive band is likely to originate from a C=O stretching of a protonated Asp or Glu side chain. Thus, it is tempting to assign this band to Asp291 serving as a counterion to the chromophore that receives a proton from the tetrapyrrole in the *in vitro* sample. The ~5 cm^{-1} upshift at pH 6.0 points to altered hydrogen bond interactions. At pH 10.0, the 1727 cm^{-1} band disappears in the *in vitro* difference spectrum, implying that the carboxyl group is deprotonated in both Pr and Pg states. Note that the assignments to the C=O stretching modes of rings **A** and **D** are consistent with the small downshifts in the IR difference spectra of *in vivo* [$^{15}N_4$]PCB-AnPixJg2 (Figure 6E of the Supporting Information). These shifts result from small admixtures of the N−H coordinates to the C=O stretching modes.

For protonated tetrapyrroles, the *B*−*C* stretching mode gives rise to the most intense IR band. In the IR difference spectra of PCB-carrying prototypical phytochromes, this mode is assigned to difference signals at 1602 (Pr) and 1586 (Pfr) cm^{-1}, in line with the calculated and observed shifts upon ^{13}C labeling and H/D exchange.[36] For deprotonated tetrapyrroles, the intensity of this mode is expected to be much lower. Accordingly, we assign this mode in the Pg/Pr difference spectrum of the *in vivo* preparation to the band pair at 1602 (Pr) and 1613 cm^{-1} (Pg) that remains largely unchanged in the pH range from 6.0 to 10.0 (Figure 3C). This assignment is consistent with the H/D shifts (−8 and −5 cm^{-1}).[36] Essentially the same results were obtained for the *in vitro* preparation of AnPixJg2 at pH 10.0, whereas at lower pH, the intensity of the (positive) Pg signal at 1613 cm^{-1} is diminished, consistent with the reduced intensity of this mode for a deprotonated chromophore. Note that like the *A*−*B* and *C*−*D* stretching modes, the *B*−*C* stretching frequency is also upshifted by ~30 cm^{-1} compared to the corresponding modes of the Pfr state of prototypical phytochromes.[36]

UV−Vis Absorption Spectroscopy. In contrast to the MAS NMR and RR spectra, the UV−vis absorption spectra display striking similarities for both *in vivo* and *in vitro* preparations at pH 7.8 (Figures 3A,E). The absorption spectra of the respective Pr forms are identical with respect to the peak positions and the band shapes, and for the Pg photoproducts, only a 7 nm (3 nm) red shift is observed for the S_0−S_1 (S_0−S_2) transition of the *in vitro*-assembled sample relative to that of the *in vivo* species. Thus, the deprotonation of the bilin ring system has only a very small effect on the electronic transitions. Larger effects are observed for the Pg state in acidic solutions, because at pH 6.0 the absorption spectrum displays a significant red-shift of 32 nm in the *in vitro* preparation (Figure 3 A,E and Figure S7 of the Supporting Information). This shift is accompanied by a decrease in oscillator strength that, as in the case of the *in vitro* Pr, reflects the decreased stability of the protein at low pH.

DISCUSSION

This study has revealed two unprecedented results. First, the *in vitro* assembly of holo-AnPixJg2 leads to structural perturbations that are primarily reflected by the bilin deprotonation in the photoproduct state. These perturbations were found to be reproducible in several preparations, suggesting that the *in vitro* assembly proceeds via a mechanism different from that of native (*in vivo*) assembly. This finding has a potential impact also for other protein−chromophore complexes and may be taken as a reminder to verify the integrity of *in vitro* assembly protocols in general. At least one other case in which *in vivo* assembly yields different properties relative to *in vitro* PCB incorporation has been reported: *in vitro* assembly of retinal to apo-bacteriorhodopsin from the retinal-deficient strain JW5 led to a substantial drop in the pK_a of the Schiff base by nearly five units compared to that of native bacteriorhodopsin.[37] The second quite surprising result, as discussed below, refers to the electronic transitions of the chromophore that are hardly affected by the deprotonation.

Structural Differences Caused by the Assembly Procedure. The "misfolding" of the *in vitro*-assembled protein has distinct consequences as they lead to tetrapyrrole deprotonation in the Pg state, which alters the electrostatics in the chromophore pocket. However, the underlying structural changes in the protein as compared to the native form are likely to be small. In the Pr state, the spectra (MAS NMR, RR, and UV−vis) of the *in vivo*- and *in vitro*-assembled holoproteins are very similar and the very few deviations noted in the RR spectra refer to weak bands that most likely involve coordinates of the pyrrole substituents. Also, the pH dependence is similar for the Pr states of the *in vivo* and *in vitro* preparations, and no chromophore deprotonation is noted at pH 10.0, unlike the PCB chromophore in the Pr state of Cph1 that releases a proton with a pK_a of ~9.3.[38]

NMR and RR spectra indicate only minor differences in the bilin structure of the Pr state between the *in vivo* and *in vitro* preparations, presumably reflecting subtle rearrangements of the chromophore in its binding pocket. In the Pg state, i.e., after a *Z*/*E* isomerization at the **C**−**D** methine bridge, these subtle changes are sufficient to cause the proton transfer from the **B**-ring pyrrole nitrogen to a proton acceptor, possibly via a decrease in the donor−acceptor distance. The most likely candidate for the proton acceptor is the side chain of Asp291, which in the Pr state is within hydrogen bonding distance of the NH groups of rings **A**−**C** (Figure 1B). In fact, the IR difference spectrum of *in vitro*-assembled AnPixJg2 shows the protonation of the side-chain carboxylate group of an aspartate residue as Pg, in contrast to the native protein. Variation of the pH has two effects on the *in vitro* Pg photoproduct: lowering the pH to 6.0 causes a substantial destabilization of the protein that goes along with a distinct red shift of the first electronic transition (Figure 3A). This spectral change occurs with a pK_a between 6 and 7. In this respect, the behavior is reminiscent of previous findings for the CBCR RcaE, also expressed in *Escherichia coli* as the present *in vitro* preparation of AnPixJg2.[39] However, RcaE acidification does not cause the protonation of the chromophore. The second and rather counterintuitive effect refers to the protonation of the chromophore at the alkaline limit, with an estimated pK_a of ~10. Clearly, this pK_a cannot directly be related to the acid−base reaction of the bilin chromophore but must refer to a protonation-dependent protein structural change that seems to partially reverse the

DOI: 10.1021/acs.biochem.5b00735
Biochemistry 2015, 54, 5839−5848

misfolding of the *in vitro*-assembled protein. As a consequence, the chromophore becomes protonated as in the native Pg state.

The techniques employed in this work do not allow the misfolded structure to be defined. However, the changes in amide I and II bands in the IR difference spectra indicate that the protein structural changes associated with the photoinduced conversion from Pr to Pg are essentially the same for the *in vivo*- and *in vitro*-assembled preparations. Moreover, these changes are rather small compared to canonical phytochromes in which major secondary structure changes are localized in the PHY domain.[19,40]

Tetrapyrrole Protonation and Electronic Transition. In previous studies, various factors that control the electronic transitions of the bilin chromophore in CBCRs were identified. Studies of model compounds[41] and CBCRs[12] suggest a substantial blue shift of the absorption occurs upon deprotonation of the chromophore. Thus, it is quite surprising that, despite a deprotonated neutral bilin ring system, the *in vitro*-assembled photoproduct reveals an absorption spectrum very similar to that of the native form, including a protonated cationic bilin. In addition, protonation of the chromophore in alkaline solutions leaves the absorption spectrum largely unchanged, whereas a red shift of the UV−vis absorption at pH 6.0 occurs without protonation of the tetrapyrrole. Although these findings refer to a state of a misfolded CBCR, they suggest that chromophore protonation is not the key parameter controlling the energy of the electronic transition of CBCRs. Note that the photoinduced reaction cycle of phytochromes typically involves a photointermediate state with a deprotonated tetrapyrrole.[42] This state, denoted "Meta-Rc" in canonical phytochromes, shows a lower oscillator strength but exhibits electronic transitions that do not differ significantly from those of the species including protonated bilins.[6,42] Thus, there must be other structural determinants for the variation of the UV−vis absorption properties.

In the case of the native AnPixJg2, some of us have previously suggested that the blue shift associated with the Pr → Pg transition is related to the influx of water molecules into the chromophore-binding pocket that is induced by a reorientation of the conserved "lid Trp" (Trp289) as a consequence of the *Z*/*E* isomerization of the chromophore.[16] The proposed correlation between chromophore hydration and the blue shift of the electronic transition ("hydration" model) was inspired by experimental findings for protonated retinal Schiff base chromophores. These chromophores display a distinct inverse relationship between the C=C stretching frequency and the absorption maximum that seems to be analogous to the striking frequency upshifts of the methine bridge stretching modes and the concomitant blue shift of the Pg absorption. However, these relationships have been established for protonated retinal Schiff bases. Thus, the decoupling between chromophore protonation and absorption maximum in the Pg state, shown in this work, now casts doubt on the "hydration" model.[16]

As an alternative to the "hydration" model, Rockwell et al.[12,13] suggested that, upon *Z*/*E* isomerization at the **C**−**D** methine bridge, ring **D** is trapped in a highly twisted orientation because of steric interactions with a conserved Phe. Thus, the length of the conjugated π-electron system is reduced and the excitation energy increased. The consequences of this trapped-twist model on the RR spectra may be estimated on the basis of a previous experimental−theoretical analysis of the Pfr state of *Pseudomonas aeruginosa*.[43] Accordingly, one would expect that an increased twist angle of ring **D** would be reflected by a frequency upshift of the *C*−*D* stretching and a downshift of the hydrogen-out-of-plane deformation (HOOP) mode. In fact, the *C*−*D* stretching mode is observed at unusually high frequencies (compared to Pfr of canonical phytochromes) for the Pg state of both the *in vivo* and *in vitro* preparations.[16] However, the HOOP mode remains in the "normal" frequency range.[16] Furthermore, solely a twist of ring **D** cannot account for the frequency upshifts of the **A**−**B** and **B**−**C** methine bridge stretching modes that are as large as that of the *C*−*D* stretching (~30 cm^{-1}). In this respect, it is interesting to refer to the recent NMR spectroscopic study of the related CBCR NpR6012g4.[15] Upon photoconversion, the most pronounced differences in the ^{13}C chemical shifts were found for C5 and C10 at the **A**−**B** and **B**−**C** methine bridges, respectively. It is, therefore, tempting to relate these findings to the unusual high frequencies of the *A*−*B* and *B*−*C* stretching modes observed in this work. Accordingly, it might be that an effective reduction of the π-electron conjugation is not restricted to the torsion at the isomerization site (**C**−**D** methine bridge) but also involves structural changes in the other methine bridges. Such an interpretation may account for these results because it does not rely upon the protonation of the chromophore. However, we cannot rule out that additional factors such as changes in the electrostatics in the chromophore environment may also contribute to the blue shift of the absorption upon the Pr → Pg transition. In any case, regardless of an extended structural change of the tetrapyrrole, one factor or even the key factor for the red/green absorption change of these CBCRs can only be decided on the basis of detailed three-dimensional structural data. Clearly, further experimental and also theoretical work is required to deepen the understanding of color control in bilin-binding proteins.

■ ASSOCIATED CONTENT

Supporting Information

The Supporting Information is available free of charge on the ACS Publications website at DOI: 10.1021/acs.biochem.5b00735.

Text, seven figures, and one table (PDF)

■ AUTHOR INFORMATION

Corresponding Authors

*E-mail: joerg.matysik@uni-leipzig.de.
*E-mail: hildebrandt@chem.tu-berlin.de.

Author Contributions

C.S. and F.V.E. contributed equally to this work.

Funding

This work was supported by the DFG (Hu702/8; SFB1078 B6), the NWO (DN 89-190 and ALW 822.02.007), and the Max-Planck-Society.

Notes

The authors declare no competing financial interest.

■ ACKNOWLEDGMENTS

We thank Prof. J. Hughes and C. Lang (Gießen) for providing labeled PCB and buffer. We are grateful to F. Lefeber and K. B. Sai Sankar Gupta (Leiden) for instrumental assistance.

DOI: 10.1021/acs.biochem.5b00735
Biochemistry 2015, 54, 5839−5848

■ ABBREVIATIONS

AnPixJg2, second GAF domain of phototaxis regulator PixJ of *Anabaena* PCC 7120; CBCRs, cyanobacteriochromes; CP-MAS, cross-polarization magic-angle spinning; Cph1Δ2, photosensory module of Cph1; CSA, chemical shift anisotropy; PCB, phycocyanobilin; PVB, phycoviolobilin; GAF, cGMP phosphodiesterase/adenylyl cyclase/FhlA; Pr, red-absorbing parental state of red/far-red phytochromes and of red/green CBCRs; Pfr, far-red-absorbing photoproduct of red/far-red phytochromes; Pg, green-absorbing photoproduct of red/green CBCRs; RR, resonance Raman; vibrational modes, *A*−*B*, *B*−*C*, and *C*−*D* denote the C=C stretching modes of the respective methine bridges; HOOP, hydrogen-out-of-plane deformation; N−H i.p., N−H in-plane bending mode.

■ REFERENCES

(1) Ernst, O. P., Lodowski, D. T., Elstner, M., Hegemann, P., Brown, L. S., and Kandori, H. (2014) Microbial and animal rhodopsins: Structures, functions, and molecular mechanisms. *Chem. Rev. 114*, 126−163.

(2) Ikeuchi, M., and Ishizuka, T. (2008) Cyanobacteriochromes: A new superfamily of tetrapyrrole-binding photoreceptors in cyanobacteria. *Photochem. Photobiol. Sci. 7*, 1159−1167.

(3) Rockwell, N. C., and Lagarias, J. C. (2010) A brief history of phytochromes. *ChemPhysChem 11*, 1172−1180.

(4) Rockwell, N. C., Martin, S. S., and Lagarias, J. C. (2012) Red/green cyanobacteriochromes: Sensors of color and power. *Biochemistry 51*, 9667−9677.

(5) Narikawa, R., Fukushima, Y., Ishizuka, T., Itoh, S., and Ikeuchi, M. (2008) A novel photoactive GAF domain of cyanobacteriochrome AnPixJ that shows reversible green/red photoconversion. *J. Mol. Biol. 380*, 844−855.

(6) Chen, Y., Zhang, J., Luo, J., Tu, J. M., Zeng, X. L., Xie, J., Zhou, M., Zhao, J. Q., Scheer, H., and Zhao, K. H. (2012) Photophysical diversity of two novel cyanobacteriochromes with phycocyanobilin chromophores: Photochemistry and dark reversion kinetics. *FEBS J. 279*, 40−54.

(7) Narikawa, R., Enomoto, G., Win, N.-N., Fushimi, K., and Ikeuchi, M. (2014) A new type of dual-Cys cyanobacteriochrome GAF domain found in cyanobacterium *Acaryochloris marina*, which has an unusual red/blue reversible photoconversion cycle. *Biochemistry 53*, 5051−5059.

(8) Xu, X.-L., Gutt, A., Mechelke, J., Raffelberg, S., Tang, K., Miao, D., Valle, L., Borsarelli, C. D., Zhao, K.-H., and Gärtner, W. (2014) Combined mutagenesis and kinetics characterization of the bilin-binding GAF domain of the protein Slr1393 from the cyanobacterium *Synechocystis* PCC6803. *ChemBioChem 15*, 1190−1199.

(9) Ishizuka, T., Kamiya, A., Suzuki, H., Narikawa, R., Noguchi, T., Kohchi, T., Inomata, K., and Ikeuchi, M. (2011) The cyanobacteriochrome, TePixJ, isomerizes its own chromophore by converting phycocyanobilin to phycoviolobilin. *Biochemistry 50*, 953−961.

(10) Narikawa, R., Ishizuka, T., Muraki, N., Shiba, T., Kurisu, G., and Ikeuchi, M. (2013) Structures of cyanobacteriochromes from phototaxis regulators AnPixJ and TePixJ reveal general and specific photoconversion mechanism. *Proc. Natl. Acad. Sci. U. S. A. 110*, 918−923.

(11) Cornilescu, C. C., Cornilescu, G., Burgie, E. S., Markley, J. L., Ulijasz, A. T., and Vierstra, R. D. (2014) Dynamic structural changes underpin photoconversion of a blue/green cyanobacteriochrome between its dark and photoactivated states. *J. Biol. Chem. 289*, 3055−3065.

(12) Rockwell, N. C., Martin, S. S., Gulevich, A. G., and Lagarias, J. C. (2014) Conserved phenylalanine residues are required for blue-shifting of cyanobacteriochrome photoproducts. *Biochemistry 53*, 3118−3130.

(13) Rockwell, N. C., Martin, S. S., Gan, F., Bryant, D. A., and Lagarias, J. C. (2015) NpR3784 is the prototype for a distinctive group of red/green cyanobacteriochromes using alternative Phe residues for photoproduct tuning. *Photochem. Photobiol. Sci. 14*, 258−269.

(14) Rockwell, N. C., Martin, S. S., Lim, S., Lagarias, J. C., and Ames, J. B. (2015) Characterization of red/green cyanobacteriochrome NpR6012g4 by solution nuclear magnetic resonance spectroscopy: A hydrophobic pocket for the C15-*E*,*anti* chromophore in the photoproduct. *Biochemistry 54*, 3772−3783.

(15) Rockwell, N. C., Martin, S. S., Lim, S., Lagarias, J. C., and Ames, J. B. (2015) Characterization of red/green cyanobacteriochrome NpR6012g4 by solution nuclear magnetic resonance spectroscopy: A protonated bilin ring system in both photostates. *Biochemistry 54*, 2581−2600.

(16) Velazquez Escobar, F., Utesch, T., Narikawa, R., Ikeuchi, M., Mroginski, M. A., Gärtner, W., and Hildebrandt, P. (2013) Photoconversion mechanism of the second GAF domain of cyanobacteriochrome AnPixJ and the cofactor structure of its green-absorbing state. *Biochemistry 52*, 4871−4880.

(17) Fukushima, Y., Iwaki, M., Narikawa, R., Ikeuchi, M., Tomita, Y., and Itoh, S. (2011) Photoconversion mechanism of a green/red photosensory cyanobacteriochrome AnPixJ: Time-resolved optical spectroscopy and FTIR analysis of the AnPixJ-GAF2 domain. *Biochemistry 50*, 6328−6339.

(18) Kufer, W., and Scheer, H. (1979) Preparation and characterization of phycobiliproteins with chromophores chemically modified by reduction. *Hoppe-Seyler's Z. Physiol. Chem. 360*, 935−956.

(19) Velazquez Escobar, F., Piwowarski, P., Salewski, J., Michael, N., Fernandez Lopez, M., Rupp, A., Muhammad Qureshi, B., Scheerer, P., Bartl, F., Frankenberg-Dinkel, N., Siebert, F., Andrea Mroginski, M., and Hildebrandt, P. (2015) A protonation-coupled feedback mechanism controls the signaling process in bathy phytochromes. *Nat. Chem. 7*, 423−430.

(20) Massiot, D., Fayon, F., Capron, M., King, I., Le Calvé, S., Alonso, B., Durand, J.-O., Bujoli, B., Gan, Z., and Hoatson, G. (2002) Modelling one- and two-dimensional solid-state NMR spectra. *Magn. Reson. Chem. 40*, 70−76.

(21) Essen, L.-O., Mailliet, J., and Hughes, J. (2008) The structure of a complete phytochrome sensory module in the Pr ground state. *Proc. Natl. Acad. Sci. U. S. A. 105*, 14709−14714.

(22) Song, C., Rohmer, T., Tiersch, M., Zaanen, J., Hughes, J., and Matysik, J. (2013) Solid-state NMR spectroscopy to probe photoactivation in canonical phytochromes. *Photochem. Photobiol. 89*, 259−273.

(23) Rohmer, T., Lang, C., Hughes, J., Essen, L.-O., Gärtner, W., and Matysik, J. (2008) Light-induced chromophore activity and signal transduction in phytochromes observed by ^{13}C and ^{15}N magic-angle spinning NMR. *Proc. Natl. Acad. Sci. U. S. A. 105*, 15229−15234.

(24) Strauss, H. M., Hughes, J., and Schmieder, P. (2005) Heteronuclear solution-state NMR studies of the chromophore in cyanobacterial phytochrome Cph1. *Biochemistry 44*, 8244−8250.

(25) Mroginski, M. A., von Stetten, D., Velazquez Escobar, F., Strauss, H. M., Kaminski, S., Scheerer, P., Günther, M., Murgida, D. H., Schmieder, P., Bongards, C., Gärtner, W., Mailliet, J., Hughes, J., Essen, L.-O., and Hildebrandt, P. (2009) Chromophore structure of cyanobacterial phytochrome Cph1 in the Pr state: Reconciling structural and spectroscopic data by QM/MM calculations. *Biophys. J. 96*, 4153−4163.

(26) Limbach, H. H., Hennig, J., Kendrick, R., and Yannoni, C. S. (1984) Proton-transfer kinetics in solids: Tautomerism in free base porphines by ^{15}N CPMAS NMR. *J. Am. Chem. Soc. 106*, 4059−4060.

(27) Falk, H., and Müller, N. (1985) On the Chemistry of Pyrrole Pigments. 60−Natural isotopic abundance ^{15}N NMR spectra of verdinoid bile pigments and their partial structures. *Magn. Reson. Chem. 23*, 353−357.

(28) Diller, A., Roy, E., Gast, P., van Gorkom, H. J., de Groot, H. J. M., Glaubitz, C., Jeschke, G., Matysik, J., and Alia, A. (2007) ^{15}N photochemically induced dynamic nuclear polarization magic-angle spinning NMR analysis of the electron donor of photosystem II. *Proc. Natl. Acad. Sci. U. S. A. 104*, 12767−12771.

DOI: 10.1021/acs.biochem.5b00735
Biochemistry 2015, 54, 5839−5848

(29) Li, S., and Hong, M. (2011) Protonation, tautomerization, and rotameric structure of histidine: A comprehensive study by magic angle-spinning solid-state NMR. *J. Am. Chem. Soc. 133*, 1534−1544.
(30) Alia, A., Matysik, J., Soede-Huijbregts, C., Baldus, M., Raap, J., Lugtenburg, J., Gast, P., van Gorkom, H. J., Hoff, A. J., and de Groot, H. J. M. (2001) Ultrahigh field MAS NMR dipolar correlation spectroscopy of the histidine residues in light-harvesting complex II from photosynthetic bacteria reveals partial internal charge transfer in the B850/His complex. *J. Am. Chem. Soc. 123*, 4803−4809.
(31) Kolodziejski, W., and Klinowski, J. (2002) Kinetics of cross-polarization in solid-state NMR: A guide for chemists. *Chem. Rev. 102*, 613−628.
(32) Wei, Y., de Dios, A. C., and McDermott, A. E. (1999) Solid-state ^{15}N NMR chemical shift anisotropy of histidines: Experimental and theoretical studies of hydrogen bonding. *J. Am. Chem. Soc. 121*, 10389−10394.
(33) Rohmer, T., Lang, C., Gärtner, W., Hughes, J., and Matysik, J. (2010) Role of protein cavity in phytochrome chromoprotein assembly and double-bond isomerization: A comparison with model compounds. *Photochem. Photobiol. 86*, 856−861.
(34) Foerstendorf, H., Benda, C., Gärtner, W., Storf, M., Scheer, H., and Siebert, F. (2001) FTIR studies of phytochrome photoreactions reveal the C═O bands of the chromophore: Consequences for its protonation states, conformation, and protein interaction. *Biochemistry 40*, 14952−14959.
(35) van Thor, J. J., Fisher, N., and Rich, P. R. (2005) Assignments of the Pfr−Pr FTIR difference spectrum of cyanobacterial phytochrome Cph1 using ^{15}N and ^{13}C isotopically labeled phycocyanobilin chromophore. *J. Phys. Chem. B 109*, 20597−20604.
(36) Schwinté, P., Foerstendorf, H., Hussain, Z., Gärtner, W., Mroginski, M. A., Hildebrandt, P., and Siebert, F. (2008) Fourier transform infrared studies of the photoinduced processes of phytochrome phyA using isotopically labelled chromophores and density functional theory calculations. *Biophys. J. 95*, 1256−1267.
(37) Kollbach, G., Steinmüller, S., Berndsen, T., Buss, V., and Gärtner, W. (1998) The chromophore induces a correct folding of the polypeptide chain of bacteriorhodopsin. *Biochemistry 37*, 8227−8232.
(38) van Thor, J. J., Borucki, B., Crielaard, W., Otto, H., Lamparter, T., Hughes, J., Hellingwerf, K. J., and Heyn, M. P. (2001) Light-induced proton release and proton uptake reactions in the cyanobacterial phytochrome Cph1. *Biochemistry 40*, 11460−11471.
(39) Hirose, Y., Rockwell, N. C., Nishiyama, K., Narikawa, R., Ukaji, Y., Inomata, K., Lagarias, J. C., and Ikeuchi, M. (2013) Green/red cyanobacteriochromes regulate complementary chromatic acclimation via a protochromic photocycle. *Proc. Natl. Acad. Sci. U. S. A. 110*, 4974−4979.
(40) Takala, H., Björling, A., Berntsson, O., Lehtivuori, H., Niebling, S., Hoernke, M., Kosheleva, I., Henning, R., Menzel, A., Ihalainen, J. A., and Westenhoff, S. (2014) Signal amplification and transduction in phytochrome photosensors. *Nature 509*, 245−248.
(41) Falk, H., and Thirring, K. (1981) Beiträge zur chemie der pyrrolpigmente—XXXVII Überbrückte gallenpigmente: N_{21}-N_{24}-methylen-aetiobiliverdin-IV-γ und N_{21}-N_{24}-methylen-aethiobilirubin-IV-γ. *Tetrahedron 37*, 761−766.
(42) Borucki, B., von Stetten, D., Seibeck, S., Lamparter, T., Michael, N., Mroginski, M. A., Otto, H., Murgida, D. H., Heyn, M. P., and Hildebrandt, P. (2005) Light-induced proton release of phytochrome is coupled to the transient deprotonation of the tetrapyrrole chromophore. *J. Biol. Chem. 280*, 34358−34364.
(43) Salewski, J., Velazquez Escobar, F., Kaminski, S., von Stetten, D., Keidel, A., Rippers, Y., Michael, N., Scheerer, P., Piwowarski, P., Bartl, F., Frankenberg-Dinkel, N., Ringsdorf, S., Gärtner, W., Lamparter, T., Mroginski, M. A., and Hildebrandt, P. (2013) The structure of the biliverdin cofactor in the Pfr state of bathy and prototypical phytochromes. *J. Biol. Chem. 288*, 16800−16814.
(44) Song, C., Psakis, G., Lang, C., Mailliet, J., Gärtner, W., Hughes, J., and Matysik, J. (2011) Two ground state isoforms and a chromophore ***D***-ring photoflip triggering extensive intramolecular changes in a canonical phytochrome. *Proc. Natl. Acad. Sci. U. S. A. 108*, 3842−3847.

DOI: 10.1021/acs.biochem.5b00735
Biochemistry 2015, 54, 5839−5848